YMTHE, Volume *28*

## Supplemental Information

# Reactive Myelopoiesis Triggered by Lymphodepleting Chemotherapy Limits the Efficacy of Adoptive T Cell Therapy

**Patrick Innamarato, Krithika Kodumudi, Sarah Asby, Benjamin Schachner, MacLean Hall, Amy Mackay, Doris Wiener, Matthew Beatty, Luz Nagle, Ben C. Creelan, Amod A. Sarnaik, and Shari Pilon-Thomas**

A

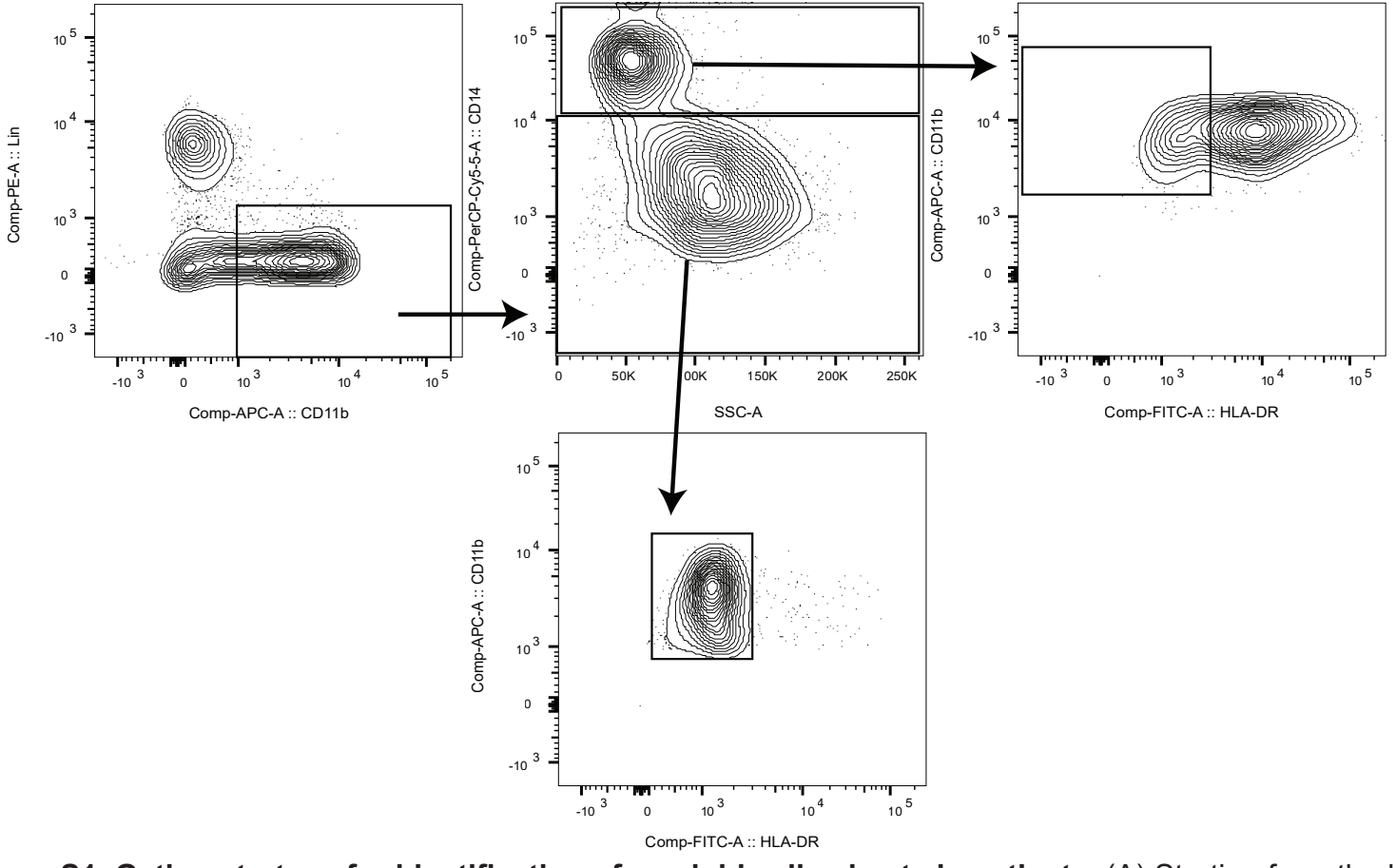


**Figure S1. Gating strategy for identification of myeloid cell subsets in patients.** (A) Starting from the left on Lin$^-$ (CD3$^-$/CD19$^-$/CD56$^-$) CD11b$^+$ cells. Arrow indicate directionality of subgates. Populations identified in Figure 1 were Lin$^-$CD11b$^+$CD14$^+$HLA-DR$^{-/low}$ (far right) and Lin$^-$CD11b$^+$CD14$^-$HLA-DR$^{-/low}$ (bottom).

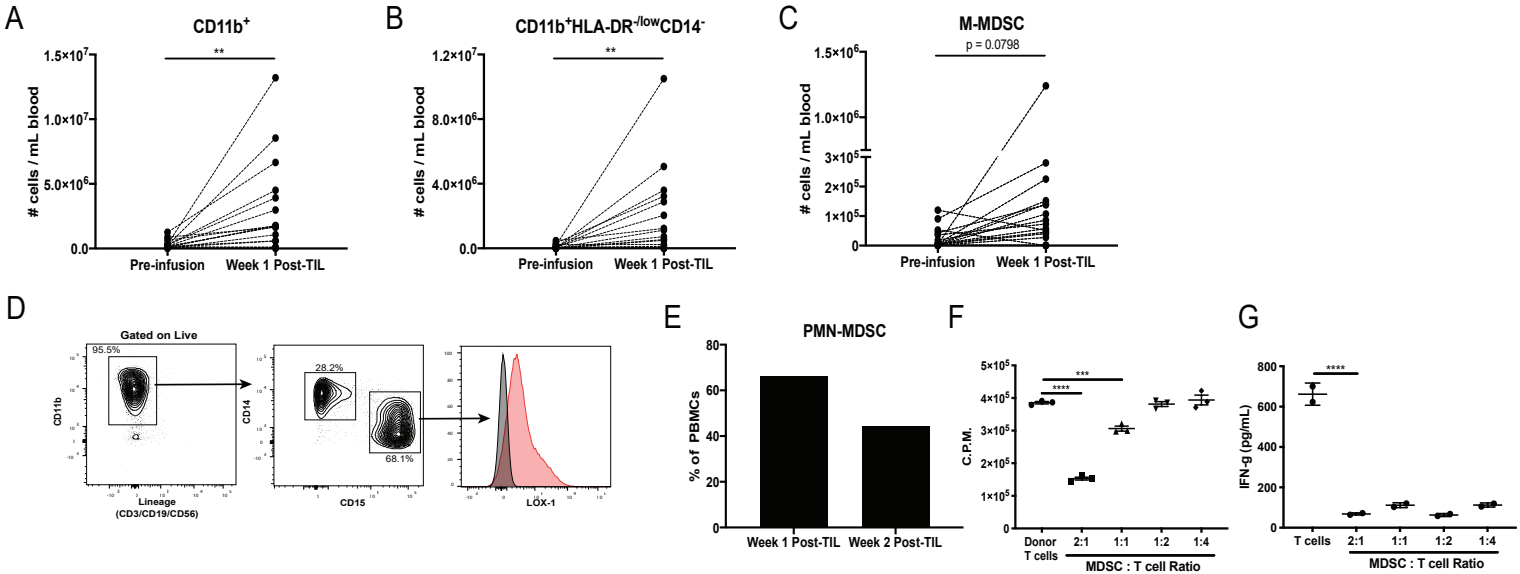


**Figure S2. Quantification and function of myeloid cells collected from melanoma patients.** (A-C) Whole cell numbers in PBMCs were determined by flow cytometry prior to and after treatment with lymphodepleting chemotherapy and TIL infusion in melanoma patients (n=21). (D) Frequency of PMN-MDSCs at Week 1 Post-TIL in a melanoma patient. (E) Frequency of PMN-MDSCs among total live PBMCs in the patient from (D) at Week 1 and Week 2 Post-TIL. (F-G) Suppression of T cell proliferation (F) and IFN-gamma production (G) were determined after 72hrs of culture of PMN-MDSCs with donor T cells. P values were determined by two-tailed t-test. Technical replicates are shown.

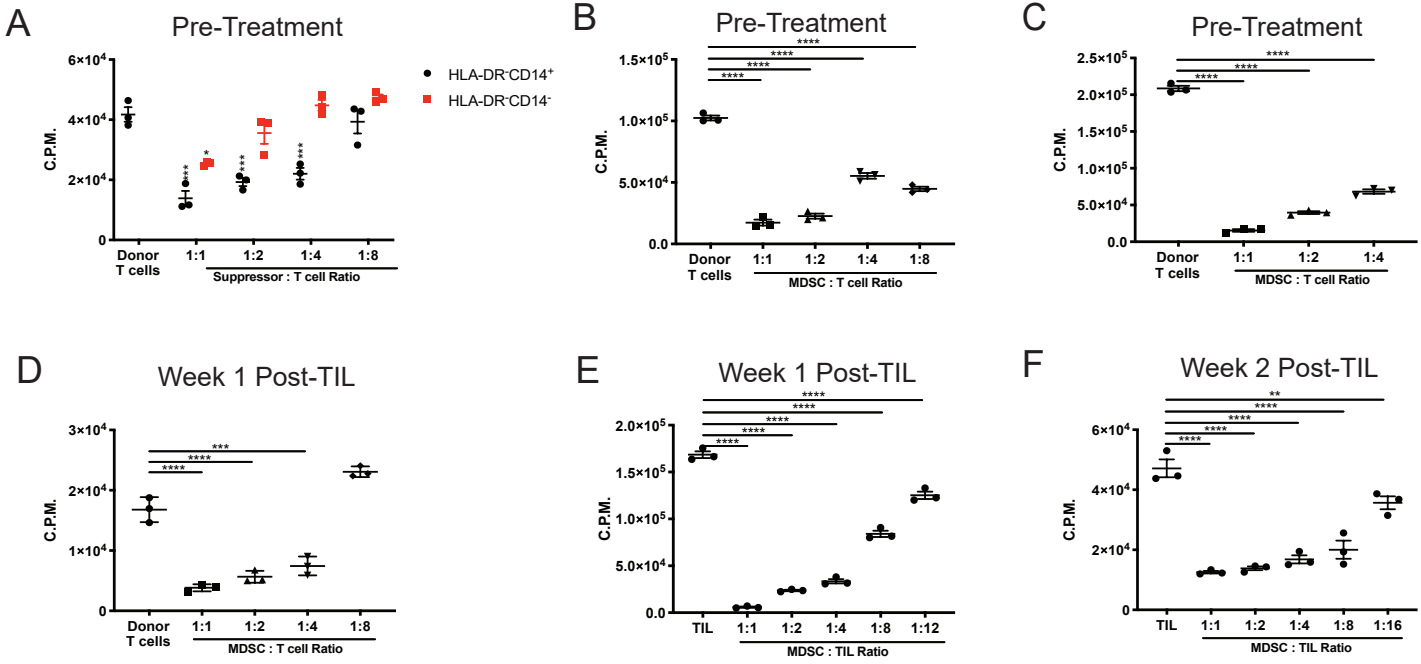


**Figure S3. Pre- and Post-treatment myeloid cells suppress donor T cells and autologous TILs.** (A-C) Donor T cells were co-cultured with myeloid cells collected from pre-treatment PBMCs. (A) HLA-DR$^-$CD14$^{+/-}$ ; (B-C) HLA-DR$^-$CD14$^+$ cells. (D-F) Suppressor assay with HLA-DR$^-$CD14$^+$ cells collected from Week 1 post-TIL infusion PBMCs were co-cultured with donor T cells (D) or autologous TIL (E-F). Myeloid cells were collected from Week 2 post-TIL infusion PBMC specimens for suppressor assay (F). P values were determined by two-tailed t-test. Technical replicates are shown.

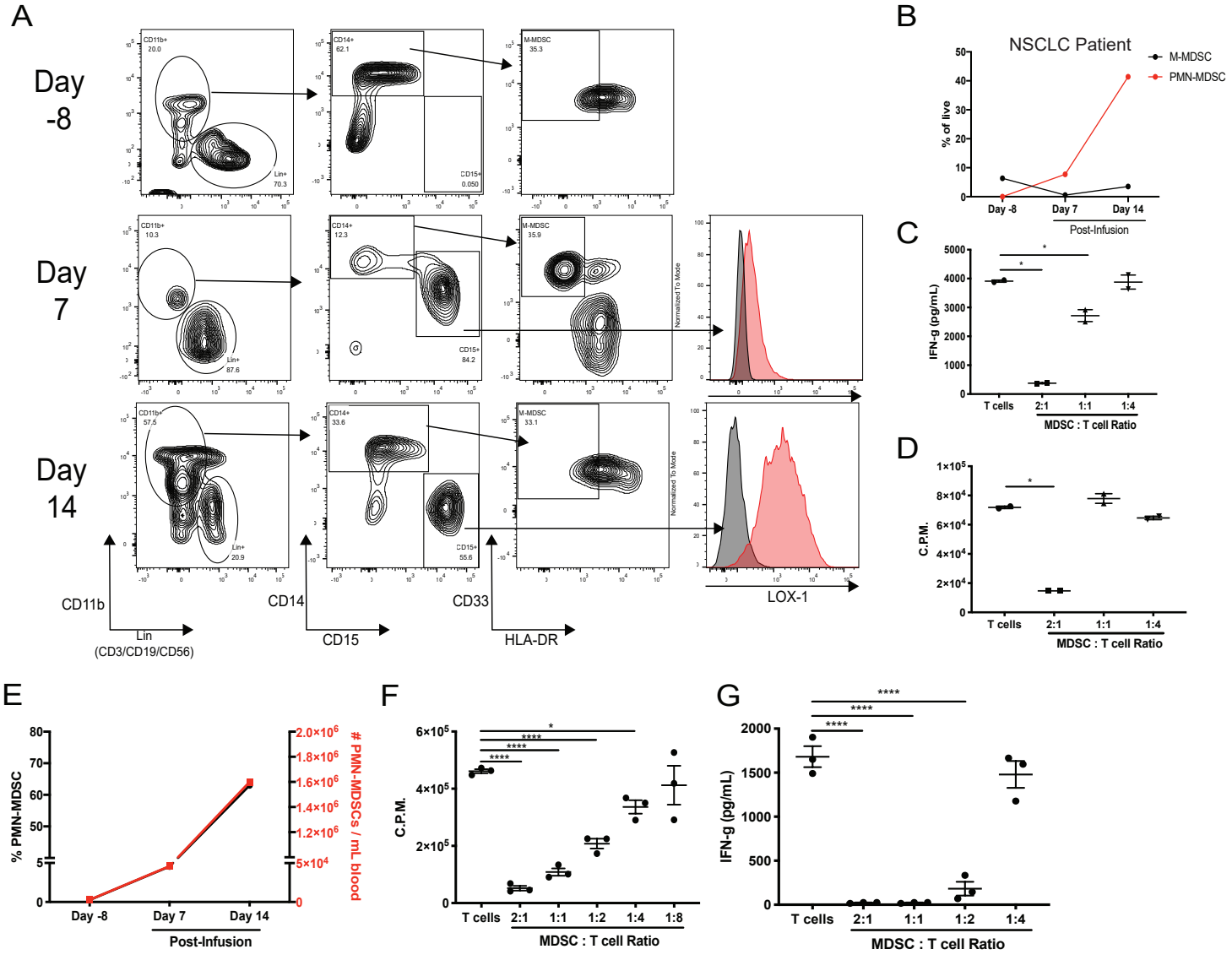


**Figure S4. Expansion of MDSCs in NSCLC patients receiving ACT with TIL.** (A) Gating strategy to identify PMN-MDSCs and M-MDSCs in NSCLC patient 1 at Day -8 before TIL infusion and Day 7 and Day 14 Post-TIL infusion and completion of a lymphodepleting chemotherapy regimen. Gates start from the percentage of live cells to subgates indicated by arrows with their respective frequency of parental gates. (B) Frequency of M-MDSCs and PMN-MDSCs of total live PBMCs at respective blood draws. (C-D) Suppression of IFN-γ production (C) and T cell proliferation (D) by PMN-MDSCs after 72hrs of co-culture. (E) Frequency of PMN-MDSCs of total live cells in NSCLC patient 2. (F-G) Suppression of T cell proliferation (F) and IFN-γ production (G) by PMN-MDSCs after 72hrs of co-culture. P values were determined by two-tailed t-test. Technical replicates are shown.

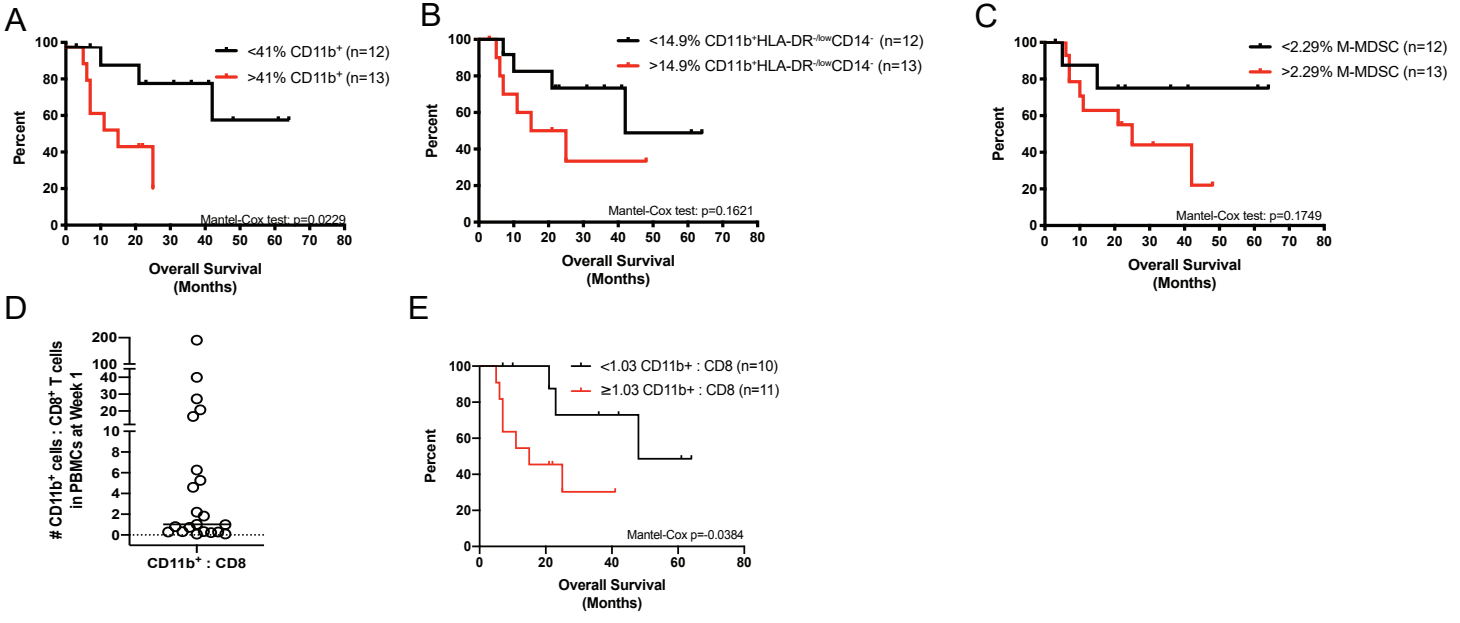


**Figure S5. Week 1 post-TIL myeloid cell frequency associations with patient survival.**
(A-C, E) Kaplan-Meier curves showing overall survival in association with the frequency of myeloid cell subsets measured in Week 1 Post-TIL PBMCs. (D) Ratio of the total number of CD11b+ cells respective to the number of CD8 T cells in Week 1 PBMCs to examine PFS (Fig. 2D) and OS in (E). Median (1.03) is indicated by the black bar (n=21 patients). Statistics are shown on each respective Kaplan-Meier plot.

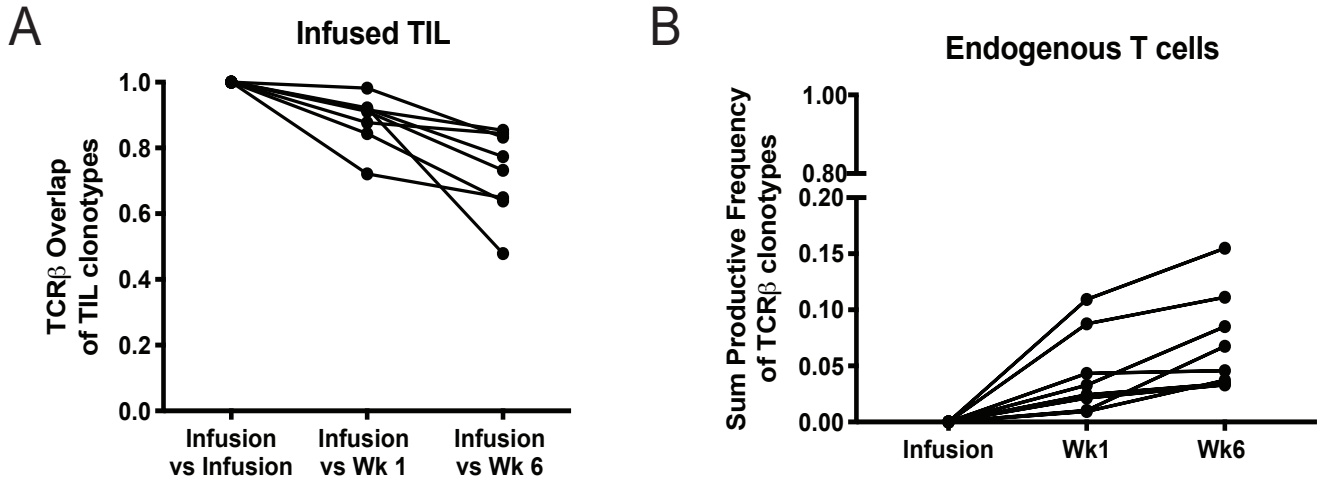


**Figure S6. Tracking TIL clonotypes and identification of endogenous T cells**
(A) TCRβ overlap of all TIL clonotypes in melanoma patients that received ACT with TIL. Overlap was compared to TILs detected from the time of infusion to Week (Wk) 1 and Wk 6 post-TIL infusion. (B) Sum frequency of all endogenous T cells that were not present within each respecitve patient's infusion product. The frequency of endogenous T cells increased over time as indicated at Wk1 and Wk6 post-TIL infusion.

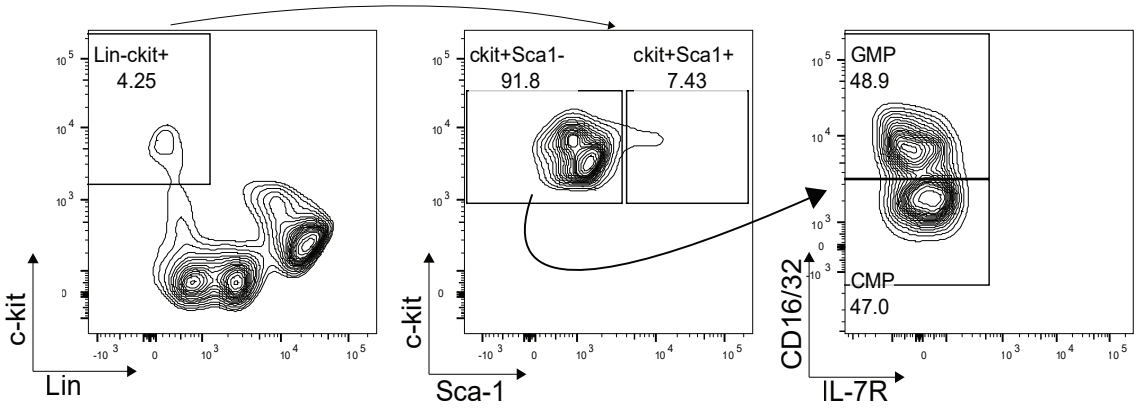


**Figure S7.** Gating strategy for HSPCs within the BM. Arrows indicate directionality of subgates, starting from the left. Lin$^{-}$c-kit$^{+}$ cells were first gated on live cells with the frequency of live indicated. Frequency in subgates are indicative of the percent of parent gates.

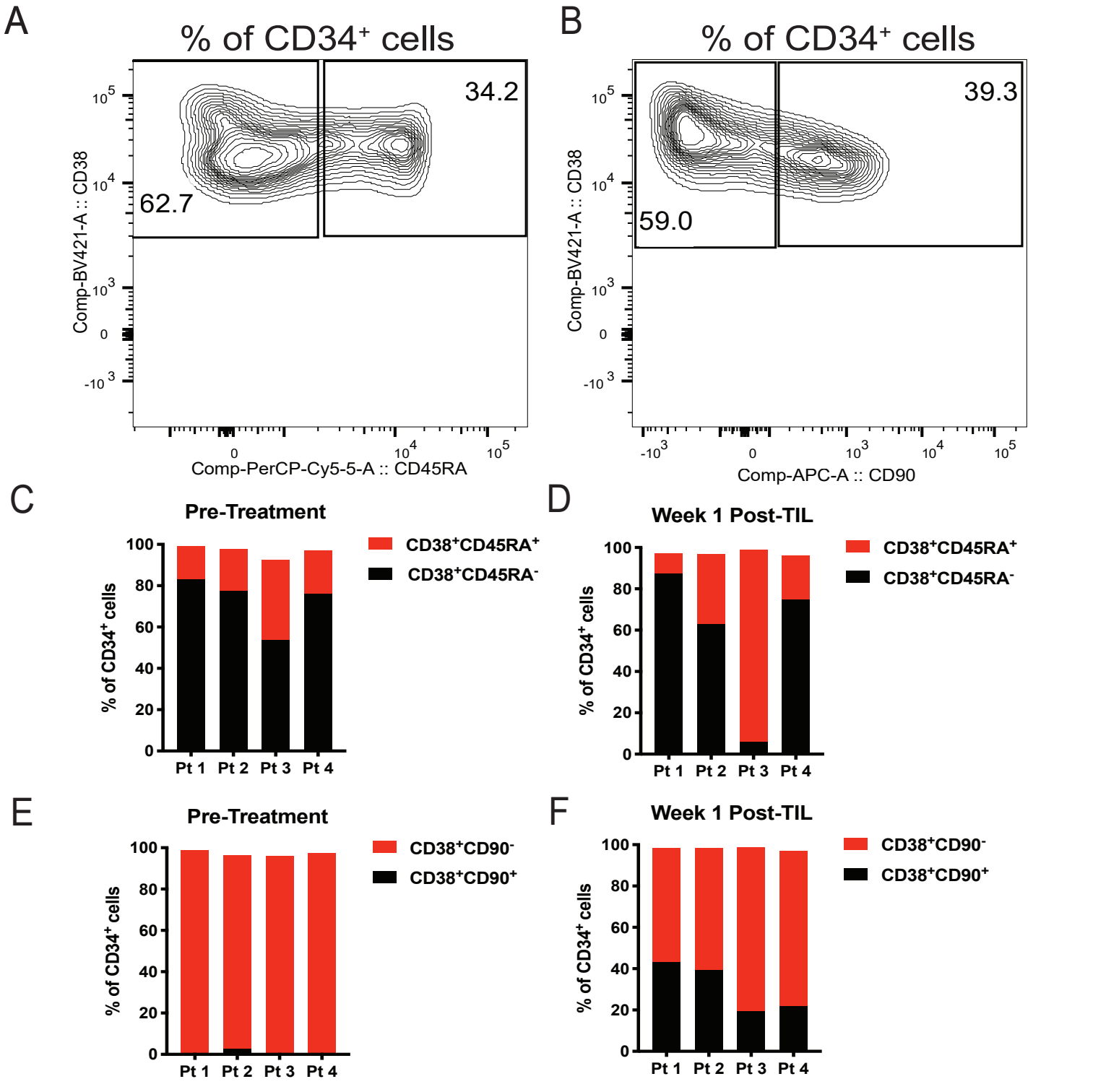


**Figure S8. Phenotype of CD34⁺ cells in melanoma patients that received ACT with TIL.** (A) CD38 and CD45RA expression in CD34⁺ cells from (Fig. 4M). (B) CD38 and CD90 expression in CD34⁺ cells from (Fig. 4M). (C-D) CD38 and CD45RA expression among CD34⁺ cells from melanoma patients in PBMCs at Pre-treatment (C) and Week 1 post-TIL (D). (E-F) CD38 and CD90 expression among CD34⁺ cells from melanoma patients at Pre-treatment with ACT and Week 1 post-TIL (F).

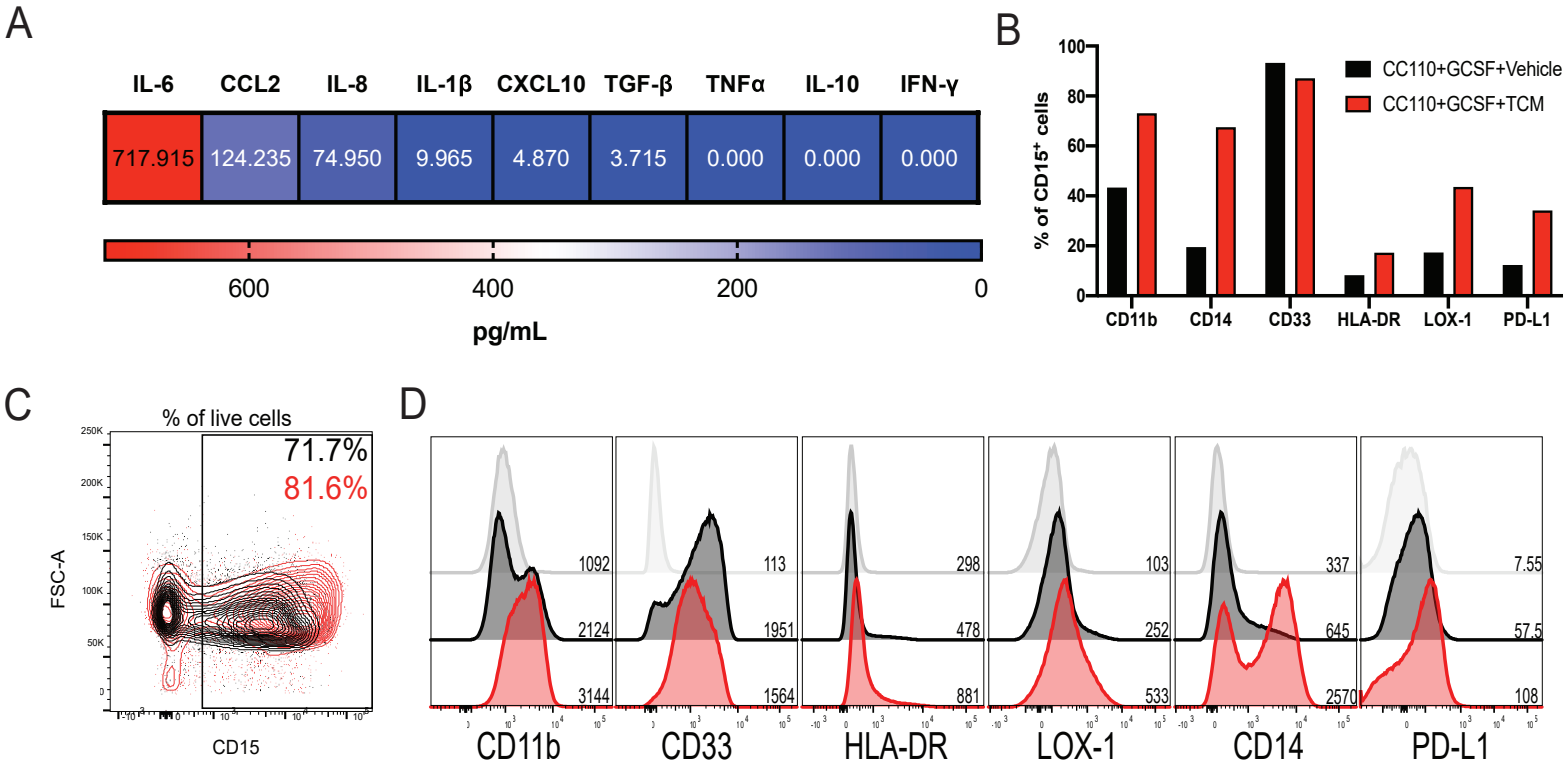


**Figure S9. Differentiation of immunosuppressive myeloid cells from lymphodepletion-mobilized CD34⁺ cells.** (A) Detection of cytokines in the TCM collected from a primary melanoma tumor cell line. (B-D) PMN suppressor cells were differentiated from CD34⁺ cells collected the Week 1 post-TIL PBMCs from a patient (Fig. 4M-N) for 14 days in CC110+GCSF. On day 10, cells were refreshed with media containing CC110+GCSF in combination with vehicle (RPMI) or TCM from (A). (B) Phenotype of CD15⁺ PMN suppressor cells differentiated from CD34⁺ cells at day 14 of differentiation protocol. (C) Frequency of CD15⁺ cells of all live cells at day 14. Black=CC110+GCSF+Vehicle, Red=CC110+GCSF+TCM. (D) Histograms of indicated myeloid cell markers. Parent gate is CD15⁺ cells as in (C). Gray = FMO, Black=CC110+GCSF+Vehicle, Red=CC110+GCSF+TCM. MFI is indicated adjacent to each histogram.

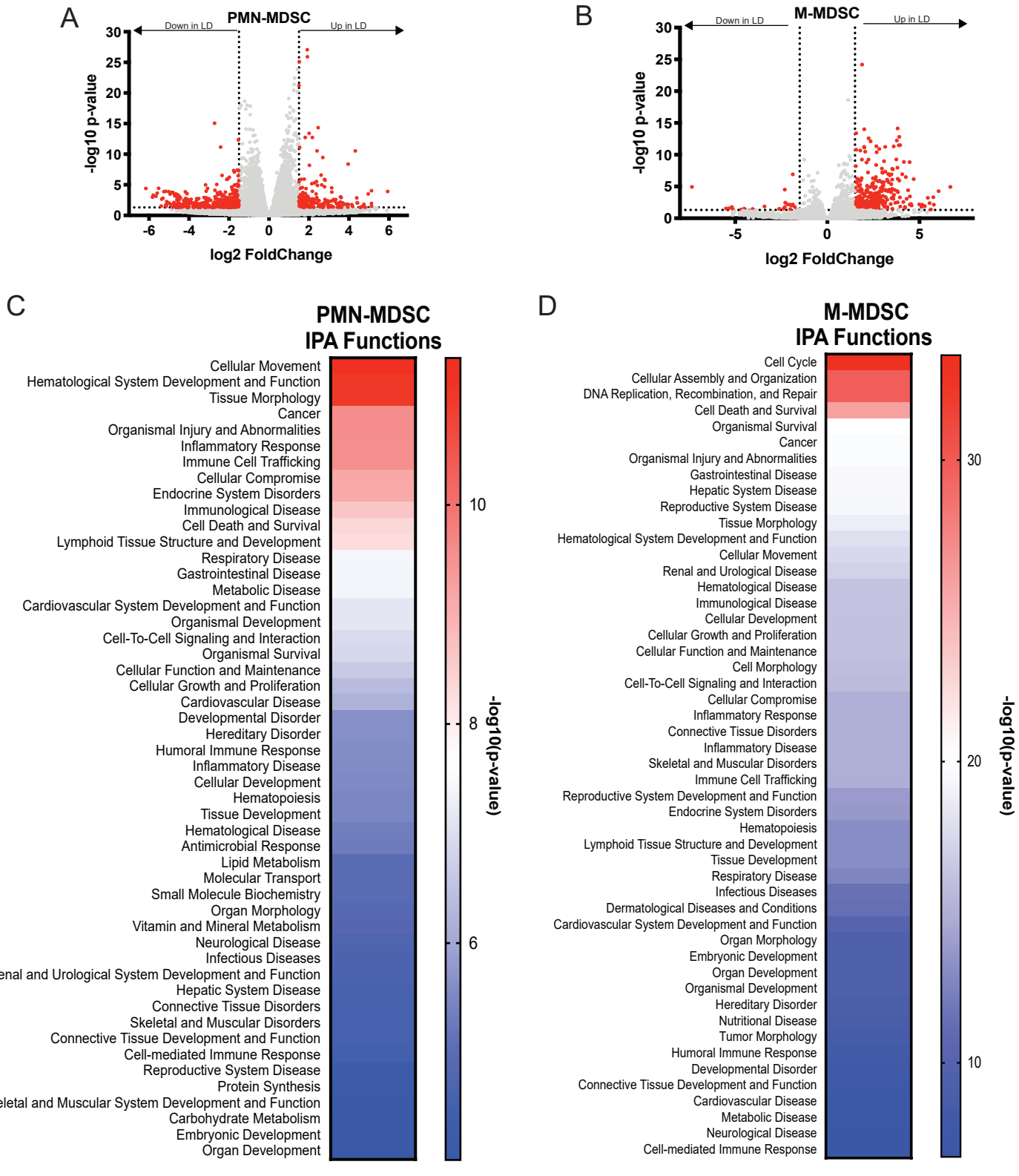


**Figure S10. RNA sequencing on MDSCs isolated from untreated and lymphodepleted tumor-bearing mice.** (A-B) Volcano plots representing significantly up- and down-regulated genes in MDSCs from LD mice. Dotted lines represent the Log2 fold change cutoff of 1.5 and -log10 p-value of p=0.05. Significant genes are shown in red; non-significant in grey. (C-D) IPA analysis of functions enriched in MDSCs from lymphodepleted mice over MDSCs from untreated tumor-bearing mice.

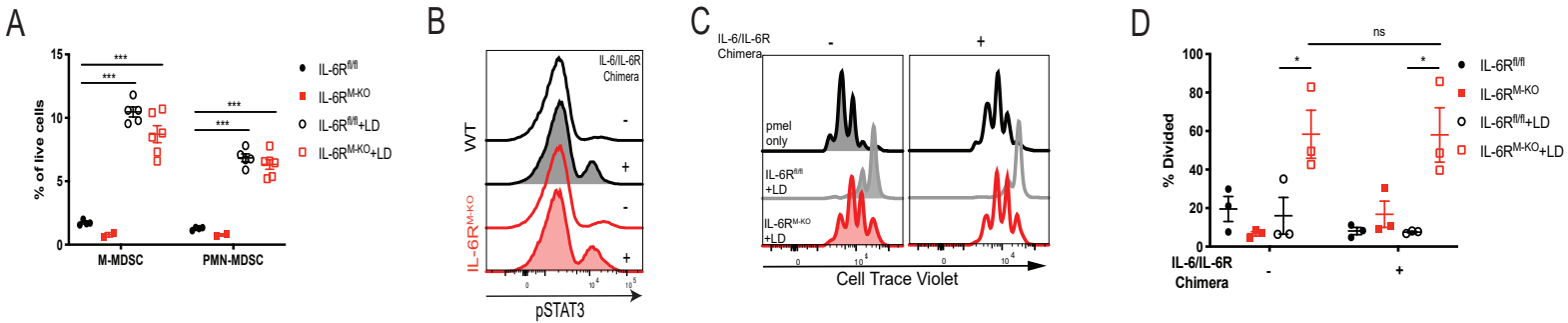


**Figure S11. MDSCs from IL-6R conditional knockout mice treated with lymphodepleting chemotherapy exhibit a reduction in their suppressive capacity.** (A) Frequency of MDSC subsets in control littermates ($IL\text{-}6R^{fl/fl}$) and knockout mice ($IL\text{-}6R^{M\text{-}KO}$) bearing B16 tumors 7 days after treatment with lymphodepleting chemotherapy. (B) IL-6/IL-6R Chimeric protein treatment rescues IL-6 signaling in knockout mice. Induction of pSTAT3 in WT MDSCs and MDSCs from $IL\text{-}6R^{M\text{-}KO}$ treated with IL-6/IL-6R Chimeric protein (200ng/mL for 30min). (C-D) MDSCs from tumor-bearing $IL\text{-}6R^{fl/fl}$ or $IL\text{-}6R^{M\text{-}KO}$ treated with or without lymphodepleting chemotherapy were collected 7 days after treatment and then cultured with Cell Trace Violet labeled pmel splenocytes and cognate peptide. MDSC and pmel co-cultures were incubated for 72hrs with or without 200ng/mL IL-6/IL-6R Chimeric protein. Pmel T cell proliferation was determined at 72hrs via Cell Trace Violet dilution. (C) Representative histogram. (D) Summary of data. P values were determined by two-tailed student t test. *=P<0.05; **=P<0.01; ***=P<0.001; ****=P<0.0001. Individual data points represent biological replicates.

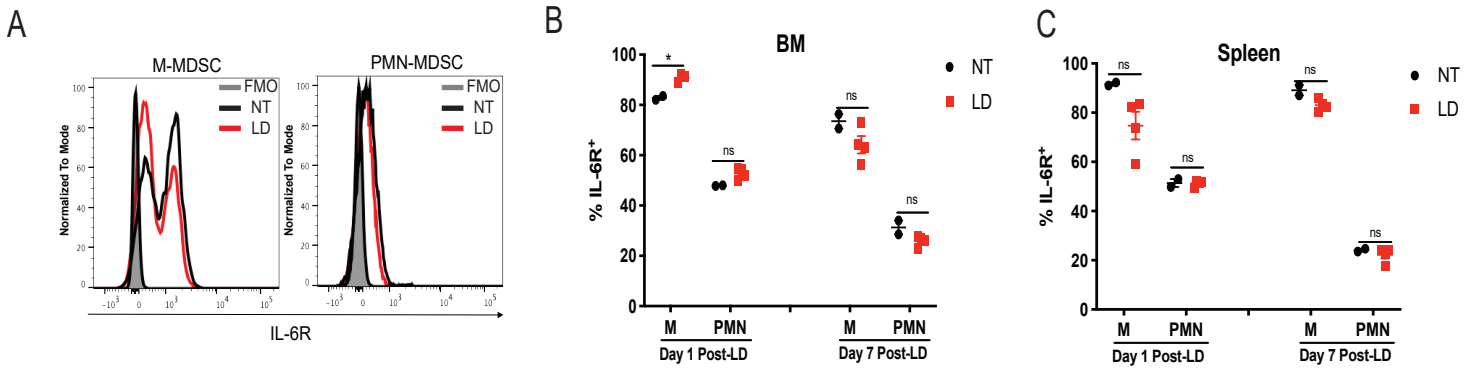


**Figure S12. IL-6R expression is not significantly altered in MDSCs from lymphodepleted mice.** (A) Representative histogram of IL-6R expression from Day 7 post-LD splenic MDSC subsets. (B-C) IL-6R expression was determined on M-MDSCs and PMN-MDSCs from NT or LD mice at indicated time points as in (Fig. 6C-D) in the BM (B) and spleen (B). Data is representative of 3 independent experiments. P values were determined by paired two-tailed t-test. *=P<0.05

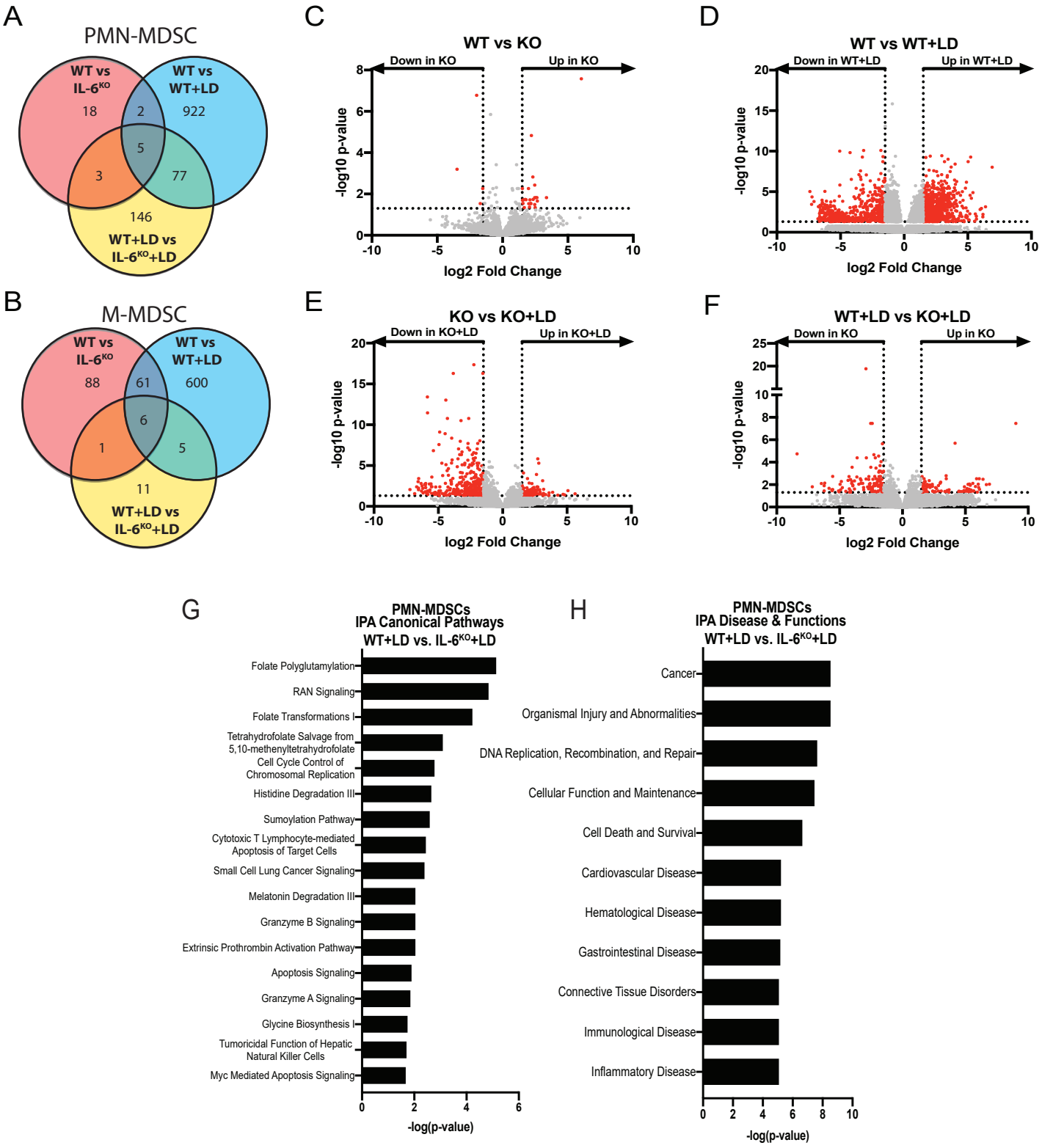


**Figure S13. RNA sequencing of WT and IL-6$^{KO}$ MDSCs from non-treated and lymphodepleted mice.** (A-B) Venn diagrams demonstrating the number of up- and down-regulated genes among each comparison and the overlap between comparisons. (C-F) Volcano plots of significantly altered genes in PMN-MDSCs comparing WT vs IL-6$^{KO}$ (C), WT vs WT+LD (D), IL-6$^{KO}$ vs IL-6$^{KO}$+LD (E), WT+LD vs IL-6$^{KO}$+LD (F). Dotted lines represent cutoffs of 1.5 fold change and log-transformed values of $p<0.05$. Significant genes are colored in red. (G-H) Ingenuity Pathway Analysis on genes enriched in WT+LD PMN-MDSCs over PMN-MDSCs from IL-6$^{KO}$ mice treated with lymphodepleting chemotherapy.

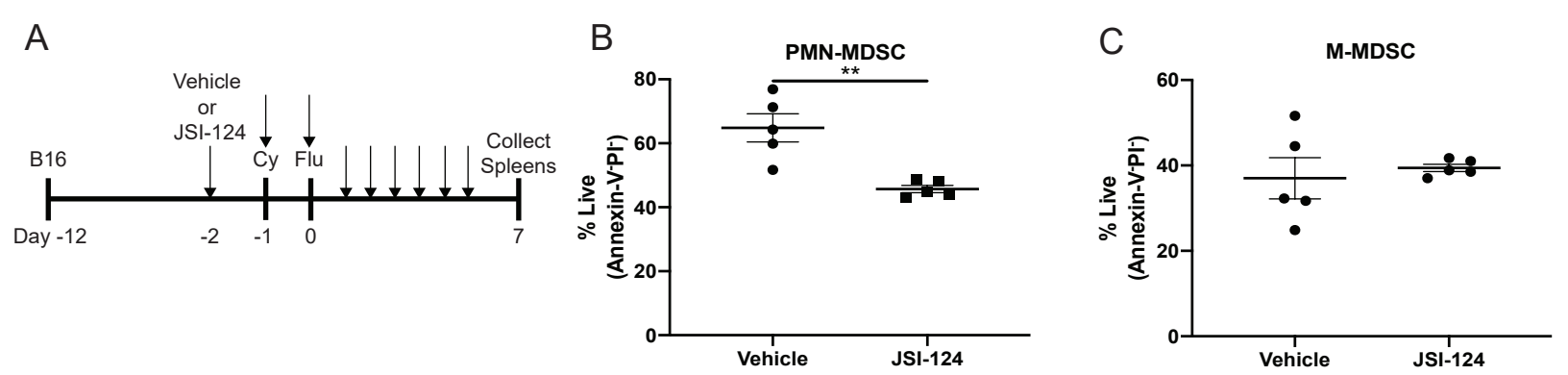


**Figure S14. In vivo JAK/STAT3 inhibition reduces PMN-MDSC survival.** (A) Experimental design for (B-C). Mice were treated with vehicle or 1mg/kg JSI-124 once daily starting 1 day prior to lymphodepleting treatment. Day 7 post-LD, MDSCs from vehicle-treated or JSI-124-treated mice were cultured for 24hrs. Live cells were determined by Annexin-V and PI negativity. (B) PMN-MDSCs; (C) M-MDSCs. P values were determined by two-tailed t-test. Data is representative of two independent experiments (n=5 mice per group).

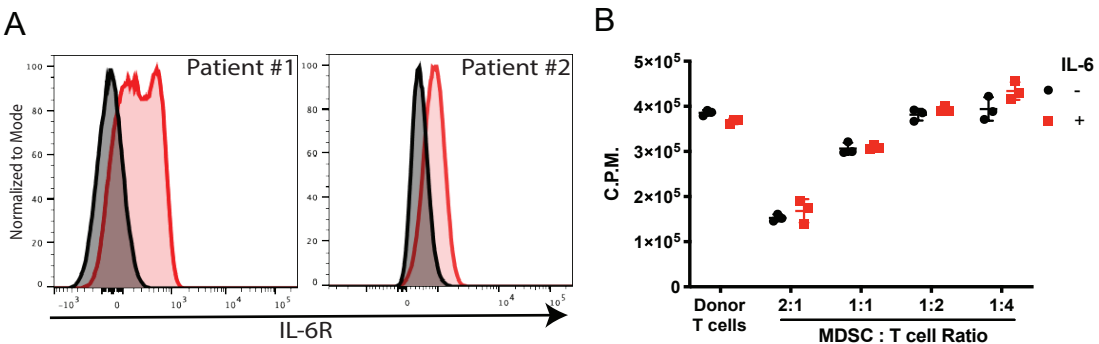


**Figure S15. Exogenous IL-6 does not alter MDSC suppressive capacity.** (A) IL-6R surface expression on PMN-MDSCs in Week 1 Post-TIL PBMCs from melanoma patient 1 (left) and melanoma patient 2 (right). (B) PMN-MDSCs purified from Week 1 Post-TIL PBMCs and co-cultured with donor T cells in media with or without 40ng/mL IL-6. T cell proliferation was determined after 72hrs of culture. P values were determined by two-tailed t-test. Technical replicates are shown.